Bioorganic & Medicinal Chemistry 25 (2017) 2754–2760

Contents lists available at ScienceDirect

Bioorganic & Medicinal Chemistry

journal homepage: www.elsevier.com/locate/bmc

Antiplasmodial activity of targeted zinc(II)-dipicolylamine complexes

Douglas R. Rice [a], María de Lourdes Betancourt Mendiola [a], Claribel Murillo-Solano [b], Lisa A. Checkley [c], Michael T. Ferdig [c], Juan C. Pizarro [b], Bradley D. Smith [a,*]

[a] Department of Chemistry and Biochemistry, 236 Nieuwland Science Hall, University of Notre Dame, Notre Dame, IN 46556, USA
[b] Department of Tropical Medicine, J Bennett Johnston Building, 1430 Tulane Avenue, Tulane University, New Orleans, LA 70112, USA
[c] Department of Biological Science, Galvin Life Sciences, University of Notre Dame, Notre Dame, IN 46556, USA

ARTICLE INFO

Article history:
Received 11 February 2017
Revised 20 March 2017
Accepted 23 March 2017
Available online 27 March 2017

Keywords:
Malaria
Antiplasmodial drugs
Zinc dipicolylamine
Fluorescence microscopy

ABSTRACT

This study measured the antiplasmodial activity of nine zinc-dipicolylamine (ZnDPA) complexes against three strains of *Plasmodium falciparum*, the causative parasite of malaria. Growth inhibition assays showed significant activity against all tested strains, with 50% inhibitory concentrations between 5 and 600 nM and almost no toxic effect against host cells including healthy red blood cells. Fluorescence microscopy studies with a green-fluorescent ZnDPA probe showed selective targeting of infected red blood cells. The results suggest that ZnDPA coordination complexes are promising antiplasmodial agents with potential for targeted malaria treatment.

1. Introduction

Malaria is the greatest parasitic killer in the world, especially in the developing regions of Asia, Africa, and South America.[1] In 2015, nearly half the world population – approximately 3.2 billion people – was at risk of contracting malaria. The disease is transmitted by female Anopheles mosquitos. The mosquito bite introduces parasites into a host's blood, which travel to the liver for maturation and reproduction. *Plasmodium falciparum* (*P. falciparum*) is the predominate species of malaria parasite, responsible for 85% of world cases.[2] Almost all existing anti-*Plasmodial* drugs, particularly 4-aminoquinoline based drugs such as chloroquine, have been rendered ineffective due to chemoresistance.[3,4] Artemisinin and related endoperoxide derivatives display the most rapid action of current drugs against *P. falciparum* infections but the appearance of artemisinin-resistant parasites in Southeast Asia threaten its efficacy.[5] Additionally, low bioavailability and poor pharmacokinetic properties diminish their therapeutic potential.[6,7] Discovering new and inexpensive treatments with novel modes of action is a top priority for improving health outcomes and controlling disease spread in endemic areas.

A promising new chemotherapeutic approach is to actively target drugs to red blood cells (RBCs) infected with *P. falciparum* parasites (iRBCs). One notable example is immuno-liposomes which have been extensively explored for drug delivery applications.[8,9] However, immuno-based strategies are limited due to antigenic variation among parasite subspecies.[10] A universal biomarker among iRBCs is the presence of an anionic outer membrane. The exterior of healthy blood cells have an electrostatic charge that is close to neutral, with zwitterionic lipids predominating on the membrane surface. However, once cells experience oxidative stress or undergo cell death, anionic phosphatidylserine (PS) becomes exposed on the external cell surface. PS is a membrane phospholipid that is exclusively localized to the inner leaflet of the lipid bilayer and promotes cell adherence with immune scavenger cells when externalized. In iRBCs, programmed erythrocyte death (eryptosis) occurs as a result of parasite growth and reproduction which scrambles membrane lipids and exposes PS on the outer membrane.[11] Exposed PS stimulates adherence to CD36 and thrombospondin receptors on vascular endothelial cells. Additionally, exposure of parasite-derived knob proteins, which act as virulence factors and mediate cytoadherence of iRBCs to endothelial cells, also contribute negative charge to the membrane surface.[12]

The feasibility of using cationic molecules to target anionic iRBC is supported by reports that quaternary ammonium salts, cationic 2-phenylbenzofurans, and dicationic 3,5-diphenylisoxazoles have *in vitro* and *in vivo* efficacy.[13–15] Many positively charged amphipathic and cysteine-rich peptides are highly toxic towards isolated sporozoites *in vitro* as well as early sporogonic stages in the mosquito midgut.[16] Also, a wide variety of transition metal chelators and organometallic complexes have been broadly screened for antimalarial activity. The most commonly explored are iron chelating agents with the aim of sequestering iron from parasites which

* Corresponding author.
E-mail address: smith.115@nd.edu (B.D. Smith).

http://dx.doi.org/10.1016/j.bmc.2017.03.050
0968-0896/

require it for reproduction. Iron-chelating drugs inhibit parasite reproduction and have been used in conjunction with traditional antimalarial drugs.[17] Ferrocene-containing compounds are particularly active against clinical isolates of both *P. falciparum* and *P. vivax*.[18,19] However, these agents may also reduce iron availability to the patient thus imparting anemic side effects. Chloroquine complexed with gold, platinum, and palladium displayed better antiplasmodial activity than chloroquine alone.[20] Auranofin, a gold-based antiarthritic drug, strongly inhibited *P. falciparum* growth *in vitro*.[21] Manganese complexes of cross-bridged tetraazamacrocyclic ligands are highly potent against *P. falciparum* strains resistant to chloroquine.[22] A number of zinc complexes with ligands such as quinine and arginine have displayed unique activity against iRBCs.[23,24] One complex in particular, zinc-desferrioxamine, was found to be more permeative into iRBCs than the desferrioxamine ligand alone as the former exchanges its bound zinc for ferric ions which enhanced uptake.[25]

Some of us have shown that fluorescent and radiolabeled zinc-dipicolylamine (ZnDPA) complexes can selectively target anionic cell surfaces in cell culture and in small animal models of disease, and used these probes for *in vivo* imaging of dead and dying mammalian cells (which expose PS) and bacterial infection (which expose anionic phosphatidylglycerol and cardiolipin).[26] Recently, we discovered that ZnDPA complexes selectively target and kill the trypanosomatid parasite *Leishmania major* (*L. major*), a causative agent of cutaneous leishmaniasis.[27] The surface of *Leishmania* parasites is negatively charged due to high fractions of anionic lipids and a thick coating of the anionic polysaccharide lipophosphoglycan. *In vivo* treatment efficacy studies showed that a ZnDPA treatment regimen significantly reduced parasite burden with minimal side effects to the local host tissue. These promising results have motivated us to determine if ZnDPA coordination complexes are active against other classes of parasites.

This study had two objectives. The first was to determine if a fluorescent ZnDPA probe was able to selectively target iRBCs and the second was to measure antiplasmodial activity in cell culture. A library of eight ZnDPA complexes was synthesized and screened for inhibitory activity against three different *P. falciparum* species that have different levels of sensitivity towards the standard antimalarial chemotherapeutic agent, chloroquine. *Plasmodium* inhibition activity was assessed using fluorescent- and tritium-based assays, and the ZnDPA complexes were concurrently screened for toxicity against models of host tissue.

2. Results and discussion

2.1. Synthesis

Shown in Scheme 1 are the ZnDPA complexes that were used in this study. The structures of complexes **1**–**5** vary in the amount of lipophilicity which was expected to influence membrane affinity. Complexes **6** and **7** were included because a previous study had shown that they have high affinities for anionic membranes.[28] The dimeric complex **8** allowed assessment of the effect gained by doubling the number of ZnDPA in one molecule. The fluorescent probe **mSeek** and control **BODIPY Dye** were prepared during previous studies.[26] The ligands **apo-1**–**apo-5** were prepared by conducting Mannich reactions with the appropriate phenol derivative having different substituents at the 4-position (Scheme 2).[29] Dimeric ligand **apo-8** was made by conducting a copper-catalyzed azide-alkyne cycloaddition (CuAAC) using **apo-5**. Mixing these water insoluble ligands with the appropriate stoichiometry of $Zn(NO_3)_2$ in methanol produced the corresponding water soluble ZnDPA complexes in quantitative yield. All com-

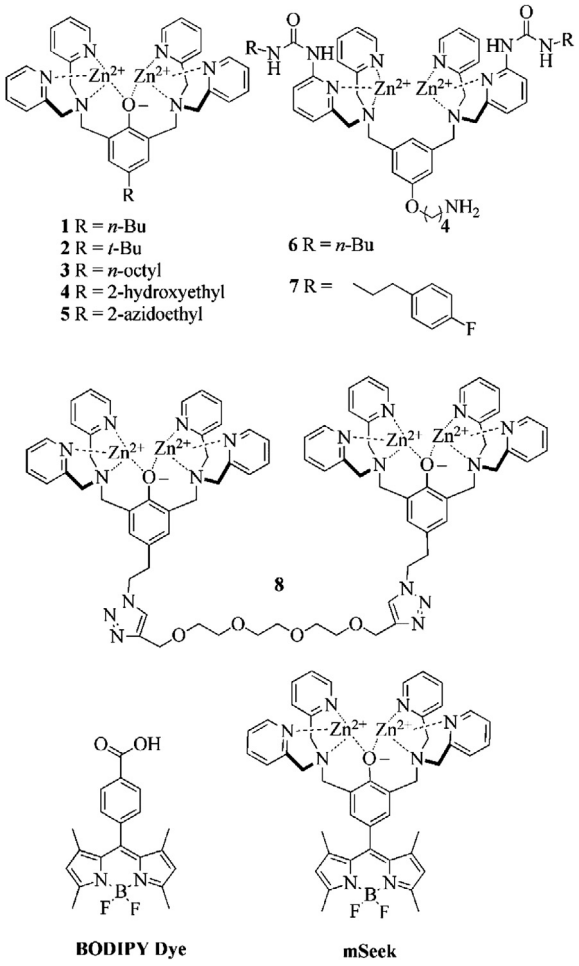

Scheme 1. Structures of compounds used in this study. All ZnDPA complexes were prepared and tested as nitrate salts.

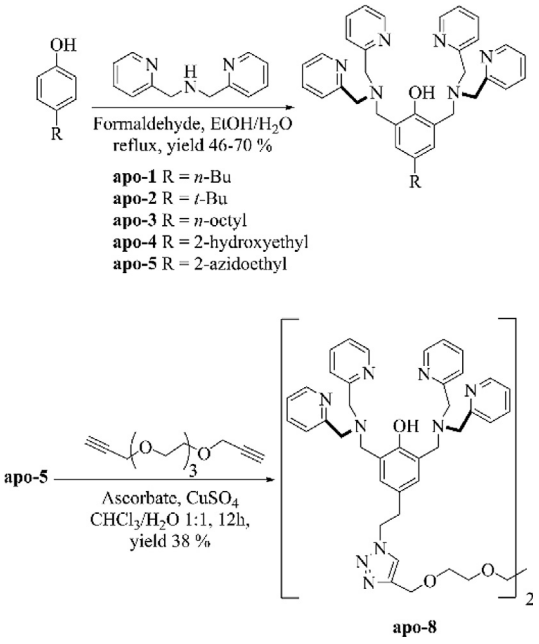

Scheme 2. Synthesis of precursor ligands.

pounds were tested as aqueous solutions except for **3**, **6** and **7** which were dissolved in 10% DMSO/water.

2.2. Fluorescence microscopy

The size of *Plasmodium* parasites depends on the developmental stage but they are approximately five times smaller than the 6–8 μM diameter of a healthy RBC. ZnDPA targeting of iRBC was explored using the green fluorescent probe **mSeek** which was shown previously to stain bacteria and *Leishmania* parasites.[27,30] Samples of red blood cells (10^4 cells per mL) infected with *P. falciparum W2* were treated with Hoechst nuclear stain which selectively localizes to iRBCs through binding parasite DNA. The same samples were co-treated with **mSeek** (5 μM) in HEPES buffer. After a 15 min incubation period, each sample was rinsed twice with fresh buffer and then subjected to fluorescence microscopy. As shown in Fig. 1A, the fraction of iRBCs is low but in each case the **mSeek** fluorescence co-localizes with the Hoechst staining of *Plasmodium* parasites. The requirement for a ZnDPA targeting ligand to selectively bind infected cells was tested by performing the same staining procedure on separate samples with a control **BODIPY Dye**. Micrographs of infected blood cells stained with the control dye displayed nonspecific staining of both infected and uninfected blood cells, with strong localization to the blood cell membrane (Fig. 1A, bottom).

To better visualize the location of **mSeek** staining, high magnification fluorescence microscopy of infected samples was performed using propidium iodide to identify iRBCs. Propidium iodide is a red-fluorescent DNA stain that is analogous to Hoechst but less susceptible to imaging artifacts due to background RBC autofluorescence. As expected, **mSeek** selectively localized to infected cells with strong accumulation at the cellular membrane (Fig. 1B). The probe also appeared to enter the cell cytoplasm and label components of the intracellular *Plasmodium* parasite. This selective affinity is likely due to the electrostatic attraction of cationic ZnDPA for exposed anionic PS on the iRBC surface. These results suggest that the ZnDPA targeting ligand can selectively identify iRBCs which may be useful for identifying or studying malaria infection in blood samples.

2.3. Antiplasmodial activity and host cell toxicity

The antiplasmodial activities of **mSeek** and ZnDPA complexes **1**–**8** were evaluated against three *P. falciparum* strains. Two strains are considered chloroquine-sensitive (*P. falciparum HB3* and *P. falciparum 3D7*) and one strain is chloroquine-resistant (*P. falciparum W2*). Parasite growth inhibition was evaluated using two different assays.[d] The inhibition of W2 and HB3 were evaluated using an incorporation assay with the tritiated nucleotide hypoxanthine ([^{3}H]Hypoxanthine). Briefly, separate cultures of P. *falciparum* were treated with a ZnDPA concentration for 48 h followed by the addition of [^{3}H]Hypoxanthine for 20 h, which is incorporated into newly replicated DNA as a quantitative measure of viable parasites for calculated growth-concentration curves (IC_{50}). The inhibition of 3D7 was evaluated using SYBR® green instead of [^{3}H]Hypoxanthine; this dye selectively binds to the minor groove of double stranded DNA which activates a green fluorescent signal upon blue excitation. The complexes were active against all strains, with IC_{50} values between ~600 and 5 nM (Figs. S19–21, Table 1). The probe **mSeek** was the most inhibitory to parasite growth, displaying an IC_{50} of 15 nM against the *P. falciparum* W2 strain and 5 nM against the HB3 strain. Among the unlabeled complexes, dimeric complex **8** displayed potent activity with IC_{50} values between 23 and 142 nM. This is potentially due to an enhanced affinity for the negatively charged iRBCs. Multimeric ZnDPA complexes have been previously shown to have higher affinity towards the anionic surfaces of dead and dying cells.[31] Nearly all the complexes were more inhibitory than chloroquine against the chloroquine-resistant W2 strain. The complexes were concurrently evaluated for host cell activity. Mammalian toxicity was assessed using a CellTiter-Blue® assay, which measures the ability of living CHO-K1 cells to convert the redox dye resazurin into an orange-fluorescent product (resorufin) (Fig. S22). Hemolytic activity was measured using the absorbance of extracellular hemoglobin released from lysed blood cells (Fig. S23). Most complexes did not display toxicity at concentrations ≤100 μM (Table 1). Complexes **1**, **2** and **mSeek** were moderately toxic with IC_{50} values between 35 and 80 μM. Complex **3** was the most toxic (IC_{50} = 17 ± 2 μM). The complexes displayed minimal hemolytic activity at concentrations ≤100 μM with the exception of complex **3** (HC_{50} = 42 ± 3 μM).

To observe parasite status following treatment, iRBCs were treated with **mSeek** (100 nM) for 24 h then stained with Giemsa followed by brightfield microscopy. Micrographs show the parasites are affected by the **mSeek** treatment. The schizont stages show abnormal morphology (Fig. 2, top). In contrast, micrographs of iRBCs treated with control **BODIPY Dye** displayed relatively healthy parasites in much greater quantity (Fig. 2, bottom) (see Figs. S24 and S25 for expanded views of multiple micrographs). At this point in time, the antiplasmodial mechanism of ZnDPA complexes remains unknown, but a few relevant points are worth highlighting. The precursor ligands are water insoluble organic compounds with very high affinities for transition metal cations such as Zn(II), Cu(II) and Fe(II/III). Conversion of the ligands to ZnDPA complexes induces water solubility and ability to selectively target the anionic membranes of iRBCs. But in-situ metal cation exchange is a possibility and the antiplasmodial activity may be due to alterations of metal cation concentrations within the blood cell cytosol. Zinc acquisition and trafficking are essential for parasite replication and a recent study demonstrated that decreasing zinc levels inhibited *Plasmodium* development.[32] Alternatively, ZnDPA binding may be destabilizing the parasite membrane or anionic DNA scaffold causing parasite death. The anionic iRBC membrane may also be targeted and disrupted which could inhibit the extracellular exit of parasites from host cells.

The World Health Organization recommends treating malaria with artemisinin combination therapy (ACT), consisting of artemisinin and another drug. Malaria strains resistant to ACT have already emerged in Southeast Asia, demonstrating the need for new drugs with novel modes of action.[1] ZnDPA complexes may be useful as chemotherapeutic leads that target the anionic membrane of infected cells, a ubiquitous biomarker of iRBCs, as demonstrated by fluorescence microscopy (Fig. 1). Moreover, ZnDPA-drug conjugates could selectively deliver chemotherapy to infected cells while reducing off-target accumulation. A ZnDPA-vancomycin derivative was recently used to treat antibiotic-resistant bacteria infections in mice without the development of chemoresistance.[33] In addition, ZnDPA-camptothecin conjugates have been reported to selectively target PS-exposing tumors in mice.[34]

3. Conclusion

The green-fluorescent ZnDPA probe, **mSeek**, selectively targets red blood cells infected with *P. falciparum*. *In vitro* activity assays indicate that ZnDPA complexes have significant and selective activity against *P. falciparum*, with little mammalian cell toxicity

[d] Authors from the University of Notre Dame tested inhibition of the W2 and HB3 strains using the hypoxanthine incorporation assay. Authors from Tulane University measured inhibition of their 3D7 strain using the SYBR green assay.

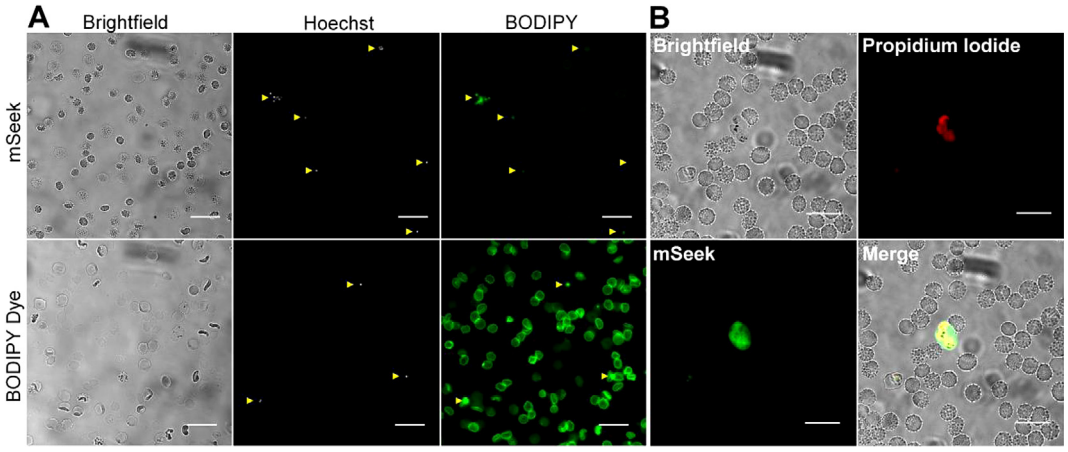

Fig. 1. [A] Representative low magnification (10×) micrographs of red blood cells infected with *P. falciparum W2* stained with Hoechst and either mSeek (*top*) or control BODIPY Dye (*bottom*) (5 μM) for 10 min prior to blue and green fluorescence imaging. The yellow arrows indicate the location of iRBCs as determined from Hoechst staining. Scale bar = 20 μm. [B] High magnification (60×) widefield micrographs of red blood cells infected with *P. falciparum W2* stained with propidium iodide and mSeek (5 μM) for 10 min prior to red and green fluorescence imaging. Scale bar = 15 μm.

Table 1
Inhibitory (IC_{50}) and hemolytic activity (HC_{50}) against mammalian cells (CHO-K1), healthy red blood cells (RBCs), and RBCs infected with *P. falciparum W2*, *HB3* and *3D7* strains. The values represent means ± standard error for 3 independent experiments.

ZnDPA Complex	*CHO-K1* IC_{50} (μM)	RBC HC_{50} (μM)	*P. falciparum*		
			W2 IC_{50} (nM)	HB3 IC_{50} (nM)	3D7 IC_{50} (nM)
mSeek	44 ± 4	>100	15 ± 3	5 ± 2	n.m.*
BODIPY Dye	88 ± 4	>100	>100	>100	n.m.*
1	38 ± 1	>100	394 ± 49	135 ± 10	251 ± 11
2	78 ± 2	>100	221 ± 75	103 ± 8	196 ± 21
3	17 ± 2	42 ± 3	527 ± 88	195 ± 39	436 ± 23
4	>100	>100	347 ± 73	290 ± 28	567 ± 23
5	>100	95 ± 4	217 ± 64	540 ± 91	205 ± 91
6	>100	>100	198 ± 31	89 ± 34	424 ± 26
7	>100	>100	161 ± 52	50 ± 12	360 ± 30
8	>100	>100	79 ± 14	23 ± 3	142 ± 34
Chloroquine	n.m.*	n.m.*	488 ± 69	96 ± 8	52 ± 12

* n.m. = not measured.

or red blood cell hemolytic activity. Further studies are warranted to determine the mechanism of action and *in vivo* performance.

4. Experimental

4.1. Synthesis and characterization

All starting materials were reagent grade purchased from commercial sources and used without further purification. NMR spectra were recorded in $CDCl_3$ with chloroform (7.26 ^{1}H, 77.0 ^{13}C) as an internal reference, using 400 MHz, 500 MHz Bruker or 600 MHz Varian spectrometers. Data are reported in the next order: chemical shift (ppm) multiplicities (s (singlet), d (doublet), t (triplet) q (quartet), m (multiplet)), coupling constants, *J* (Hz) and integration. Reactions were monitored by TLC analysis conducted in silica-gel on TLC-Al foils. The fluorescent probe **mSeek**, control **BODIPY Dye**, **6**, and **7** were prepared during previous studies.[28,30]

4.2. General procedure for ligand synthesis

The appropriate 4-substituted phenol and formaldehyde were added to a solution of di-(2-picolyl)amine (DPA) in EtOH/H_2O (12 mL/5 mL) and the mixture kept at reflux temperature for 48 h. The solvent was removed and residue partitioned between CH_2Cl_2 and H_2O. The aqueous layer was extracted with CH_2Cl_2 three times and then dried over $MgSO_4$. The crude material was purified by silica gel chromatography (CH_2Cl_2/MeOH/NH_4OH; 94/5/1) to yield the desired product.

Apo-1: yellow oil in 72% yield (682.0 mg, 1.190 mmol). ^{1}H NMR (400 MHz, $CDCl_3$) δ 10.77 (s, 1H), 8.52 (dd, *J* = 3.2, 1.5 Hz, 4H), 7.74–7.57 (m, 4H), 7.50 (d, *J* = 7.9 Hz, 4H), 7.20–7.05 (m, 4H), 7.01 (s, *J* = 5.5 Hz, 2H), 3.88 (s, 8H), 3.80 (s, *J* = 7.6 Hz, 4H), 2.50 (t, *J* = 7.6 Hz, 2H), 1.59–1.46 (m, 2H), 1.31 (td, *J* = 14.6, 7.3 Hz, 2H), 0.89 (td, *J* = 7.2, 1.0 Hz, 3H). ^{13}C NMR (101 MHz, $CDCl_3$) δ 159.4, 153.8, 148.9, 136.4, 132.5, 129.0, 123.6, 122.9, 121.9, 77.3, 59.8, 54.9, 34.7, 33.9, 22.3, 14.0. HRMS-ESI [M+H$^+$] *m*/*z* 573.3336: calcd for $C_{36}H_{41}N_6O$ 573.3337.

Apo-2: pale yellow crystals in 63% yield (600 mg, 1.05 mmol). ^{1}H NMR (400 MHz, $CDCl_3$) δ 8.54–8.49 (m, 4H), 7.59 (td, *J* = 7.6, 1.8 Hz, 4H), 7.50 (d, *J* = 7.8 Hz, 4H), 7.19 (s, *J* = 9.7 Hz, 2H), 7.11 (ddd, *J* = 7.3, 4.9, 1.1 Hz, 4H), 3.88 (s, 8H), 3.81 (s, 4H), 1.25 (s, 9H). ^{13}C NMR (101 MHz, $CDCl_3$) δ 159.3, 153.5, 148.8, 140.9, 136.4, 125.9, 123.2, 122.9, 121.9, 59.9, 55.2, 33.9, 31.6. HRMS-ESI [M+H$^+$] *m*/*z* 573.3336: calcd for $C_{36}H_{41}N_6O$ 573.3337.

Apo-3: yellow oil in 90% yield (687.0 mg, 1.09 mmol) ^{1}H NMR (400 MHz, $CDCl_3$) δ 8.49 (d, *J* = 4.2 Hz, 4H), 7.56 (tt, *J* = 7.8, 3.9 Hz, 4H), 7.47 (d, *J* = 7.8 Hz, 4H), 7.08 (dd, *J* = 6.6, 5.6 Hz, 4H), 6.98 (s, 1H), 3.85 (s, *J* = 8.7 Hz, 8H), 3.77 (s, *J* = 8.7 Hz, 4H), 2.46 (dd, *J* = 17.8, 10.0 Hz, 2H), 1.51 (dd, *J* = 14.4, 7.0 Hz, 2H), 1.23 (d, *J* = 14.2 Hz, 10H), 0.83 (t, *J* = 6.8 Hz, 3H). ^{13}C NMR (101 MHz, $CDCl_3$) δ 159.4, 153.7, 148.9, 136.4, 132.6, 129.0, 123.7, 122.9, 121.9, 77.3,

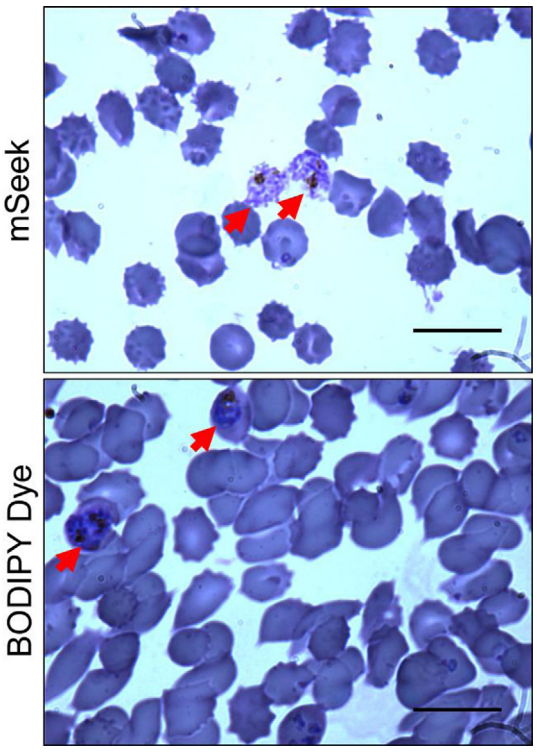

Fig. 2. Brightfield microscopy of *P. falciparum 3D7* infected red blood cells treated with mSeek (*top*) or control BODIPY Dye (*bottom*) (100 nM) for 24 h followed by Giemsa staining. Red arrows indicate iRBCs. Scale bar = 15 μm.

59.8, 54.9, 35.1, 31.9, 31.7, 29.5, 29.3, 29.2, 22.6, 14.1. HRMS-ESI [M+H$^+$] *m*/*z* 629.3962: calcd for $C_{40}H_{49}N_6O$ 629.3963.

Apo-4: yellow pale solid in 65% yield (660 mg, 1.18 mmol). ^{1}H NMR (500 MHz, $CDCl_3$) δ 8.41 (d, *J* = 4.2 Hz, 4H), 7.49 (td, *J* = 7.7, 1.7 Hz, 4H), 7.38 (d, *J* = 7.8 Hz, 4H), 7.03 (dd, *J* = 6.7, 5.3 Hz, 6H), 6.98 (s, 2H), 3.86 (s, 8H), 3.79–3.68 (m, 6H), 2.68 (t, *J* = 6.5 Hz, 2H). ^{13}C NMR (126 MHz, $CDCl_3$) δ 158.1, 154.3, 148.6, 136.6, 130.3, 128.7, 123.1, 122.9, 122.1, 77.4, 63.2, 59.4, 55.0, 38.3. HRMS-ESI [M+H$^+$] *m*/*z* 561.2963: calcd for $C_{34}H_{37}N_6O_2$ 561.2963.

Apo-5: yellow solid 45% yield (419.0 mg). ^{1}H NMR (400 MHz, $CDCl_3$) δ 8.48 (d, *J* = 4.2 Hz, 4H), 7.55 (td, *J* = 7.7, 1.7 Hz, 4H), 7.44 (d, *J* = 7.8 Hz, 4H), 7.07 (dd, *J* = 6.8, 5.5 Hz, 4H), 7.02 (s, 2H), 3.85 (s, 8H), 3.77 (s, 4H), 3.74 (s, 1H), 3.38 (t, *J* = 7.2 Hz, 2H), 2.75 (t, *J* = 7.2 Hz, 2H). ^{13}C NMR (101 MHz, $CDCl_3$) δ 159.1, 154.8, 148.9, 136.5, 129.5, 127.6, 124.2, 123.0, 122.0, 100.5, 63.6, 59.8, 54.8, 52.8, 34.6. HRMS-ESI [M+H$^+$] *m*/*z* 586.3037: calcd for $C_{34}H_{36}N_9O$ 586.3038.

Apo-8: **Apo-5** (126.0 mg, 0.215 mmol) and 4,7,10,13-tetraoxahexadeca-1,15-diyne (23.2 mg, 0.102 mmol) were dissolved in $CHCl_3$ (3 mL). Then, $CuSO_4{\cdot}5H_2O$ (103.0 mg, 0.645 mmol) and sodium L-ascorbate (128.0 mg, 0.645 mmol) were mixed in a separated vial and added to the reaction mixture. The mixture was stirred overnight. The crude was washed with saturated aqueous solution of Na_4EDTA and saturated aqueous NaCl. The organic layer was dried over magnesium sulfate and concentrated under reduced pressure. The crude was purified by chromatography to yield the product in 38% yield (27.8 mg, 0.02 mmol). ^{1}H NMR (500 MHz, MeOD) δ 8.38 (d, *J* = 4.9 Hz, 4H), 7.90 (s, 2H), 7.77–7.69 (m, 12H), 7.65 (d, *J* = 7.8 Hz, 4H), 7.39 (t, *J* = 7.8 Hz, 4H), 7.26–7.19 (m, 4H), 6.99 (s, 2H), 6.85 (d, *J* = 7.3 Hz, 4H), 6.77 (s, 4H), 6.41 (d, *J* = 8.2 Hz, 4H), 3.97 (t, *J* = 6.0 Hz, 4H), 3.76–3.67 (m, 12H), 3.54 (d, *J* = 16.0 Hz, 16H), 1.81 (ddd, *J* = 19.6, 14.1, 6.8 Hz, 8H). ^{13}C NMR (126 MHz, MeOD) δ 169.8, 160.9, 160.4, 158.2, 149.3, 141.6, 139.7, 138.6, 135.2, 133.3, 124.5, 124.0, 123.7, 122.4, 114.9, 112.7, 108.4, 79.5, 68.2, 60.8, 60.8, 59.7, 38.5, 27.7, 26.2. HRMS-ESI [M+H$^+$] *m*/*z* 1397.7207: calcd for $C_{80}H_{89}N_{18}O_6$ 1397.7207.

4.3. Zinc complexation

Stock solutions of bis(di-2-picolyl)amine ligands and $Zn(NO_3)_2{\cdot}6H_2O$ were prepared in methanol (each 25 mM) and appropriate aliquots were mixed such that the [Zn^{2+}]:[DPA] molar ratio was 1:1. The solutions were stirred for 1 h before the solvent was removed and the residue held under vacuum for 1 h. Each residue was dissolved in water or 10% DMSO/water in the case of **3**, **6** and **7** to give a stock solution of each ZnDPA complex.

4.4. Hypoxanthine incorporation growth inhibition assay

P. falciparum strains W2 (Indochina) and HB3 (Honduras) were maintained in O-positive human red blood cells (BioChemed, Winchester, VA) and RPMI 1640 medium (Gibco) supplemented with 0.5% Albumax II (Gibco), 0.25% sodium bicarbonate (Corning), and 0.01 mg/mL gentamicin (Gibco) under an atmosphere of 90% N_2, 5% O_2, and 5% CO_2. Cultures underwent at least two life cycles prior to initiation of assays to ensure that normal growth was established. Dose-response curves were generated using a hypoxanthine incorporation assay.[35] Briefly, parasite cultures for assays were maintained as asynchronous cultures and required to reach a parasitemia of no less than 1%, with 70% of parasites in the early ring stage. Sample parasitemia and hematocrit were then adjusted to 0.2% and 2%, respectively, and the samples were added to test plates containing ZnDPA complexes. The appropriate control solution (water or 10% DMSO/water) were added to control wells. Parasites were exposed to drug dilutions for 48 h. [^{3}H] hypoxanthine (PerkinElmer) was added to the plates and incubated for an additional 20 h before freezing at ~80 °C for ~24 h. Plate contents were harvested and counted on a Trilux beta counter. The dose-response curves show means for three independent biological replicates.

4.5. SYBR® Green and Giemsa staining

The *P. falciparum* 3D7 (Netherland/Africa)[36] and W2 (Indochina) strains were maintained in continuous culture in RPMI-1640 medium (Gibco Grand Island, NY, USA) supplemented with 10% heat-inactivated non-immune AB human serum, 26 mg/L of hypoxanthine (Sigma-Aldrich St. Louis, MO, USA) and 10 mg/L of Gentamicin (Gibco). Uninfected O-positive erythrocytes (Interstate Blood Bank, Memphis, TN) in a 50% suspension were added every two days to maintain the hematocrit at 5%. Cultures were incubated at 37 °C in 5% O_2 and 5% CO_2 atmosphere with daily change of culture medium. Final dilutions of chloroquine (Sigma-Aldrich, St Louis, MO) were prepared in water. 96-well flat-bottom plates were coated with 10 μL of 11 different dilutions of each compound in duplicate in the following range: CQ (3.12–3200 nM); ZnDPA complexes (4.88–5000 nM).

A parasite suspension of each strain with parasitemia at 0.5% (ring form higher than 80% of the total stage form) and hematocrit 1.5% was added (190 μL per well) to the microplates pre-dosed with ZnDPA and then incubated at 37 °C in an atmosphere of 5% O_2 and 5% CO_2 for 72 h. For control parasites wells, appropriate 10 μL aliquots of water or 10% DMSO/water were added. After incubation, the plates were freeze-thawed at −80 °C and growth inhibition was determined using a SYBR® Green I-based method as previously described.[37,38] Briefly, 100 μL of freeze-thaw homogenate were transferred to 96-well black plates. 100 μL of SYBR® Green lysis buffer I (2× SYBR® Green I, Thermo Fisher Scientific), Tris-HCl (100 mM, pH 7.5), EDTA (10 mM), Saponin (0.016% w/v), and Triton X-100 (1.6% v/v) were added to each well. The plates

were incubated in darkness at room temperature for 1 h. The fluorescence was measured using a fluorescence plate reader (Synergy HT, Biotek Instruments, Inc., Winooski, VT, USA) at 485 nm wavelength using Gen 5 2.01 software. The 50% inhibitory concentrations (IC_{50}) were calculated using the online program ICEstimator 1.2 (http://www.antimalarial-icestimator.net/).[39] IC_{50} values were acceptable only if the ratio of fluorescence intensity between the parasite at concentration 0 versus FU at maximum concentration, was equal or higher than 2.

Morphological assessment of 3D7 parasites after treatment with **mSeek** or control **BODIPY dye** was performed using a Giemsa staining procedure. A 200 μL suspension of parasites at a parasitemia of 1% and a hematocrit of 1.5% was exposed at 100 nM of **mSeek** or **BODIPY dye** for a 24 h period. After exposure, the parasite samples were stained with Giemsa using a 10% w/v aqueous solution for 15 min. Micrographs were acquired using an Olympus BX41 microscope with a 100x objective and QIClic CCD Camera (QImaging).

4.6. Fluorescence microscopy

Samples of *P. falciparum W2* infected RBCs were aliquoted into 1.5-mL microcentrifuge tubes, followed by centrifugation (500 rpm, 5 min). The infected RBCs were resuspended in 1 mL of sterile Phosphate Buffered Saline (PBS, 10 mM PO_4^{3-}, 145 mM NaCl, 2.6 mM KCl, pH 7.4) and treated for 15 min with ZnDPA probe **mSeek** or a control **BODIPY dye** (Abs max: 499 nm; Em max: 520 nm) (5 μM). The samples were also stained with either Hoechst 33342 nuclear stain (Hoechst) or propidium iodide (PI). Hoechst-stained samples were co-treated with **mSeek** or control **BODIPY dye** using a 20 mM stock solution (Thermo Fischer Scientific) to reach a final concentration of 1 μM in the sample for 15 min. Samples stained with PI were permeabilized with a PBS solution containing 0.01% saponin prior to incubation with PI (Sigma-Aldrich, 5 μM) for 30 min. The samples were washed twice with fresh buffer to reduce background fluorescence, dispersed into fresh solution, and then aliquoted onto glass slides. Micrographs were acquired using a Nikon Eclipse TE2000-U epifluorescence microscope with a 10× or 60× objective and a Photometrics Cascade 512B CCD. Fluorescence images were captured using UV (excitation, 340/80 nm; emission, 435/85 nm), GFP (450/90, 500/50), and Cy5 (620/60, 700/75) filter sets.

4.7. Mammalian cell culture and toxicity

Chinese hamster ovary cells (CHO-K1) were purchased from the American Type Culture Collection (CCL-61). Cells were grown to a confluence of 85% in F-12K media supplemented with 10% FBS and 1% streptavidin L-glutamate at 37 °C and 5% CO_2. 10^5 cells/mL were seeded in a 96-well plate and incubated in the presence of increasing concentrations of ZnDPA complex for 72 h at 37 °C, along with the appropriate solvent controls. Afterward, 20 μL of CellTiter-Blue reagent was added to 100 μL of the cell culture, followed by a 4-h incubation period at 37 °C, and the fluorescence was measured (excitation, 555 nm; emission, 580 nm) using a Typhoon FLA 9500 laser scanner (GE Healthcare) and analyzed with ImageQuant TL software (GE Healthcare). The output fluorescence values were background subtracted from wells containing medium alone and normalized to wells containing untreated cells. Normalized fluorescence values were plotted against the ZnDPA complex concentration using GraphPad Prism 5 software.

4.8. Red blood cell (RBC) lysis

RBC lysis was measured using a literature procedure.[40] Briefly, O-positive human red blood cells (BioChemed, Winchester, VA) were centrifuged at 500*g* for 5 min, then the plasma was aspirated and discarded. The RBCs were washed two times with a 150 mM NaCl solution followed by replacement with PBS at pH 7.4. Aliquots (100 μL) of RBCs suspended in PBS were added to 96 well plates. Increasing concentration of each ZnDPA complex was added to the wells in triplicate. For positive control wells, 10 μL of 20% Triton X-100 were added. For negative control wells, 10 μL of 10% DMSO/water were added. The plates were incubated at 37 °C and continuously rocked for three hours. After incubation, the plates were centrifuged for 5 min at 500*g* to pellet intact erythrocytes. Using a multichannel pipet, 100 μL of supernatant from each well were carefully transferred into clear, flat-bottomed 96-well plates. The supernatant absorbance (λ = 450 nm) was measured using a SpectraMax Plus 384 Microplate Reader (Molecular Devices). Each sample was background subtracted from negative control wells and normalized to positive control wells which represent 100% hemolysis.

Acknowledgments

We are grateful for funding support from the NIH (RO1GM059078 to B. D. S. and T32GM075762 to D. R. R.), COLCIENCIAS (Programa de Formación Doctoral "Francisco José de Caldas – Convocatoria 512 to C. M. S.), Tulane University (Startup funds to J. C. P.) and Technical Support from the University of Notre Dame, the Notre Dame Integrated Imaging Facility, the Harper Cancer Research Institute Imaging and Flow Cytometry Core Facility, and the Freimann Life Sciences Center. The authors declare no financial conflict of interest.

A. Supplementary data

Supplementary data associated with this article can be found, in the online version, at http://dx.doi.org/10.1016/j.bmc.2017.03.050.

References

1. World Malaria Report 2015. Geneva, Switzerland: WHO; 2015. 2015.
2. Cullen KA, Arguin PM. Malaria surveillance–United States, 2012. *MMWR Surveill Summ*. 2014;63:1–22.
3. Le Bras J, Musset L, Clain J. Antimalarial drug resistance. *Med Mal Infect.*. 2006;36:401–405.
4. *Global Report on Antimalarial Drug Efficacy and Drug Resistance: 2000–2010*2010. Geneva, Switzerland: WHO; 2010.
5. Amaratunga C, Lim P, Suon S, et al. Dihydroartemisinin-piperaquine resistance in *Plasmodium falciparum* malaria in cambodia: A multisite prospective cohort study. *Lancet Infect. Dis.*. 2016;16:357–365.
6. Titulaer HA, Zuidema J, Kager PA, Wetsteyn JC, Lugt CB, Merkus FW. The pharmacokinetics of artemisinin after oral, intramuscular and rectal administration to volunteers. *J Pharm Pharmacol*. 1990;42:810–813.
7. Augustijns P, D'Hulst A, Van Daele J, Kinget R. Transport of artemisinin and sodium artesunate in caco-2 intestinal epithelial cells. *J Pharm Sci*. 1996;85:577–579.
8. Urban P, Estelrich J, Adeva A, Cortes A, Fernandez-Busquets X. Study of the efficacy of antimalarial drugs delivered inside targeted immunoliposomal nanovectors. *Nanoscale Res Lett*. 2011;6:620.
9. Moles E, Urban P, Jimenez-Diaz MB, et al. Immunoliposome-mediated drug delivery to *Plasmodium*-infected and non-infected red blood cells as a dual therapeutic/prophylactic antimalarial strategy. *J Controlled Release*. 2015;210:217–229.
10. Recker M, Buckee CO, Serazin A, et al. Antigenic variation in *Plasmodium falciparum* malaria involves a highly structured switching pattern. *PLoS Pathog*. 2011;7:e1001306.
11. Eda S, Sherman IW. Cytoadherence of malaria-infected red blood cells involves exposure of phosphatidylserine. *Cell Physiol Biochem*. 2002;12:373–384.
12. Tokumasu F, Ostera GR, Amaratunga C, Fairhurst RM. Modifications in erythrocyte membrane zeta potential by *Plasmodium falciparum* infection. *Exp Parasitol*. 2012;131:245–251.
13. Oh SS, Chishti AH, Palek J, Liu SC. Erythrocyte membrane alterations in *Plasmodium falciparum* malaria sequestration. *Curr Opin Hematol*. 1997;4:148–154.
14. Bakunov SA, Bakunova SM, Wenzler T, et al. Synthesis and antiprotozoal activity of cationic 2-phenylbenzofurans. *J Med Chem*. 2008;51:6927–6944.

15. Patrick DA, Bakunov SA, Bakunova SM, et al. Synthesis and *in vitro* antiprotozoal activities of dicationic 3,5-diphenylisoxazoles. *J Med Chem*. 2007;50:2468–2485.
16. Vizioli J, Salzet M. Antimicrobial peptides versus parasitic infections? *Trends Parasitol.*. 2002;18:475–476.
17. Aguiar AC, Santos Rde M, Figueiredo FJ, et al. Antimalarial activity and mechanisms of action of two novel 4-aminoquinolines against chloroquine-resistant parasites. *PLoS ONE*. 2012;7:e37259.
18. Biot C, Nosten F, Fraisse L, Ter-Minassian D, Khalife J, Dive D. The antimalarial ferroquine: from bench to clinic. *Parasite*. 2011;18:207–214.
19. Roux C, Biot C. Ferrocene-based antimalarials. *Future. Med Chem*. 2012;4:783–797.
20. Navarro M, Castro W, Madamet M, Amalvict R, Benoit N, Pradines B. Metal-chloroquine derivatives as possible anti-malarial drugs: evaluation of anti-malarial activity and mode of action. *Malar. J.*. 2014;13:471.
21. Sannella AR, Casini A, Gabbiani C, et al. New uses for old drugs. Auranofin, a clinically established antiarthritic metallodrug, exhibits potent antimalarial effects *in vitro*: mechanistic and pharmacological implications. *FEBS Lett*. 2008;582:844–847.
22. Hubin TJ, Amoyaw PN, Roewe KD, et al. Synthesis and antimalarial activity of metal complexes of cross-bridged tetraazamacrocyclic ligands. *Bioorg Med Chem*. 2014;22:3239–3244.
23. Ogunlana OO, Ogunlana OE, Ademowo OG. Antiplasmodial activity of quinine-zinc complex and chloroquine: a comparative *in vitro* assessment. *Afr. J. Pharm. Pharmacol.*. 2012;6:516–519.
24. Malhotra P, Dasaradhi PV, Mohammed A et al., Use of Selected Amino Acid-Zinc Complexes as Anti-Malarials, *US Patent Application,* US 20050090480 A1.
25. Chevion M, Chuang L, Golenser J. Effects of zinc-desferrioxamine on *Plasmodium falciparum* in culture. *Antimicrob Agents Chemother*. 1995;39:1902–1905.
26. Rice DR, Clear KJ, Smith BD. Imaging and therapeutic applications of zinc(II)-dipicolylamine molecular probes for anionic biomembranes. *Chem Commun*. 2016;52:8787–8801.
27. Rice DR, Vacchina P, Norris-Mullins B, Morales MA, Smith BD. Zinc(II)-dipicolylamine coordination complexes as targeting and chemotherapeutic agents for leishmania major. *Antimicrob Agents Chemother*. 2016;60:2932–2940.
28. Plaunt AJ, Harmatys KM, Wolter WR, Suckow MA, Smith BD. Library synthesis, screening, and discovery of modified zinc(II)-bis(dipicolylamine) probe for enhanced molecular imaging of cell death. *Bioconjugate Chem*. 2014;25:724–737.
29. Lubben M, Feringa BL. New method for the synthesis of nonsymmetric dinucleating ligands by aminomethylation of phenols and salicylaldehydes. *J Org Chem*. 1994;59:2227–2233.
30. Rice DR, Gan H, Smith BD. Bacterial imaging and photodynamic inactivation using zinc(II)-dipicolylamine bodipy conjugates. *Photochem Photobiol Sci*. 2015;14:1271–1281.
31. Smith BA, Harmatys KM, Xiao S, et al. Enhanced cell death imaging using multivalent zinc(II)-bis(dipicolylamine) fluorescent probes. *Mol. Pharmaceutics.*. 2013;10:3296–3303.
32. Marvin RG, Wolford JL, Kidd MJ, et al. Fluxes in "free" and total zinc are essential for progression of intraerythrocytic stages of *Plasmodium falciparum*. *Chem Biol*. 2012;19:731–741.
33. Yarlagadda V, Sarkar P, Samaddar S, Haldar J. A vancomycin derivative with a pyrophosphate-binding group: a strategy to combat vancomycin-resistant bacteria. *Angew Chem Int Ed Engl*. 2016;55:7836–7840.
34. Tsou LK, Liu Y-W, Chen Y-Y, et al. Zinc-dipicolylamine directed pharmaceutical delivery system (zaps) as an innovative cancer drug delivery platform. *Cancer Res*. 2015;75. 4413-4413.
35. Desjardins RE, Canfield CJ, Haynes JD, Chulay JD. Quantitative assessment of antimalarial activity *in vitro* by a semiautomated microdilution technique. *Antimicrob Agents Chemother*. 1979;16:710–718.
36. Su XZ. Tracing the geographic origins of *Plasmodium falciparum* malaria parasites. *Pathog. Global Health.*. 2014;108:261–262.
37. Bacon DJ, Latour C, Lucas C, Colina O, Ringwald P, Picot S. Comparison of a sybr green I-based assay with a histidine-rich protein II enzyme-linked immunosorbent assay for *in vitro* antimalarial drug efficacy testing and application to clinical isolates. *Antimicrob Agents Chemother*. 2007;51:1172–1178.
38. *In vitro* Module, *P. falciparum* drug sensitivity assay using sybr® green I assay technique, WWARN, 2011.
39. Le Nagard H, Vincent C, Mentre F, Le Bras J. Online analysis of *in vitro* resistance to antimalarial drugs through nonlinear regression. *Comput Methods Programs Biomed*. 2011;104:10–18.
40. Evans BC, Nelson CE, Yu SS, et al. Ex vivo red blood cell hemolysis assay for the evaluation of pH-responsive endosomolytic agents for cytosolic delivery of biomacromolecular drugs. *J. Visualized Exp.* 2013;e50166.